Electronic Supplementary Material (ESI) for Journal of Materials Chemistry A.

Supporting Information

Highly Loading Metal Atoms on Graphdiyne for Efficient Nitrogen Fixation to Ammonia

Yan Fang,[a,c] Yurui Xue,*[a,b] Lan Hui,[a,c] Xi Chen[a,c] and Yuliang Li*[,a,c]

Materials and methods

Materials

Hexabromobenzene and tetrabutylammonium fluoride (TBAF) were purchased from J&K Scientific and Alfa Aesar, respectively. $MnSO_4 \cdot H_2O$ was provided by Energy Chemical. Tetrahydrofuran (THF) and toluene were refluxed with sodium for several hours to remove residual water before applied in reaction. The other reagents were all used as received without any extra purification treatment unless specifically mentioned. Water used in this experiment was purified with a Millipore system.

Preparation of graphdiyne nanosheets (GDY NSs)

GDY NSs were synthesized via an acetylenic cross-coupling reaction. Several nitric acid-treated carbon cloths (CC) and copper foils were immersed in pyridine solution and kept for 2 h at 80 ℃. 50 mL 0.6 mg mL^{-1} hexaethynylbenzene (HEB) solution dissolved in pyridine was added dropwise in 5 h into above solution and then the whole system was kept at 110 ℃ for 24 h under Ar atmosphere. It is noted that the reaction setup should be kept protection from light. After reaction, GDY NSs grown on CC substrate were taken out from the reactor and washed with dimethylformamide (DMF), acetone successively, and immersed in 0.5 M H_2SO_4 for at least 12 h. Finally, the samples were washed with deionized water and ethanol and dried in air.

Preparation of Mn_{SA}/GDY

A piece of freshly prepared GD NSs grown on CC was used as the cathode and immersed in 0.5 M H_2SO_4 containing 50 mM $MnSO_4 \cdot H_2O$ to allow sufficient adsorption of Mn species. Electrochemical deposition was performed under galvanostatic condition at a current density of 10 mA cm^{-2} for 1800s on CHI 660E electrochemical Workstation. The obtained Mn_{SA}/GDY was washed with deionized water and ethanol successively, dried at 30 ℃ in vacuum and kept in Ar atmosphere before electrochemical tests.

Charaterizations

Scanning electron microscopy (SEM) images were obtained using an S-4800 field emission scanning electron microscope. Transmission electron microscopy (TEM), high-resolution transmission electron microscopy (HRTEM) and energy dispersive X-ray spectroscopy (EDX) tests were all carried out through a JEM-2100F electron microscope. High-angle annular dark-field scanning transmission electron microscopy (HAADF-STEM) images were obtained on the aberration-corrected cubed FEI Titan Cubed Themis G2 300 or JEM-ARM200F (JEOL, Tokyo, Japan) TEM/STEM operated at 200 kV with cold filed-emission gun and double hexapole Cs correctors (CEOS GmbH, Heidelberg, Germany). The attainable spatial resolution defined by the probe-forming objective lens is better than 80 pm. X-ray diffraction (XRD) was conducted on the Rigaku D/max-2500 rotation anode X-ray diffractometer using Cu Kα radiation (λ =1.54178 Å). Raman spectroscopy was obtained through a Renishaw-2000 Raman spectrometer with a 473 nm excitation laser source. X-ray photoelectron spectroscopy (XPS) measurement was conducted on a Thermo Scientific ESCALab 250Xi instrument with monochromatic Al Kα.

Electrochemical tests

All the electrochemical measurements were carried out on CHI 660E electrochemical Workstation (CHI. 660D, Shanghai CH. Instruments, China). A gas purification set-up was equipped to conduct the electrochemical nitrogen reduction reaction (NRR) experiment. The electrochemical nitrogen reduction reaction was performed in a carefully cleaned H-type two-compartment cell separated by Nafion 117 membrane under ambient conditions. The Nafion 117 membranes used in this experiment were protonated by boiling in water for 1 h, in H_2O_2 for 1 h and then in water for another 1 h, followed by being boiled in 0.5 M H_2SO_4 for 3 h and in water for 6 h before measurement. All the boiling steps above were performed at 80 °C. Before each measurement, the feeding gas was carefully purified through a Cu-trap to remove possible impurities such as NO_x and other nitrogen compounds in order to eliminate the contributions of contaminates. 0.1 M N_2-saturated Na_2SO_4 aqueous solution was freshly prepared as the electrolyte, the as-synthesized samples were directly used as the working electrode, the saturated calomel electrode (SCE) was used as the reference electrode, and the graphitic rod was used as the counter electrode. The NRR was performed for 1 h at each potential with high-purity N_2 continuously bubbled to the surface of samples and then the electrolyte was collected for products detection and the sample was washed carefully. The NRR tests were repeated for 3 times at each applied potential in repetitive tests. The operations of argon

control experiments were the same as nitrogen reduction experiments except from the feeding gas. As for cycling stability test, electrolytes were collected at an interval of 1 h so as to detect ammonia products. The cell and tested samples were rinsed with deionized water for several times in order to remove purities and absorbed ammonia on the surface. And then the cleaned samples were immersed in fresh electrolytes again for the next electrochemical cycle.

Detection and quantification of ammonia

The electrochemical synthesized ammonia was detected through indophenol blue method. The calibration curve was determined as follows: 4 mL standard NH_4Cl solutions with series of concentrations in 0.1 M Na_2SO_4 were mixed with 50 μL oxidizing solution [NaClO (ρCl = 4~4.9) solution containing 0.75 M NaOH], 500 μL coloring solution (aqueous solution of 0.4 M $C_7H_5O_3Na$ and 0.32 M NaOH) and 50 μL catalytic solution (aqueous solution of 1% $Na_2[Fe(NO)(CN)_5]\cdot 2H_2O$) successively. UV-vis measurements were carried out within a range of 800 nm to 500 nm after standing at ambient conditions for 1 h. The calibration curve was obtained from the absorbance at 660 nm and calculated as: $y = 0.0921x + 0.004$, $R^2 = 0.999$.

Ammonia yield (Y_{NH3}) was determined using the following equation:

$$Y_{NH3} = \left(C_{NH3} \times V\right) / \left(t \times m\right)$$

Where C_{NH3} is the detected concentration of ammonia, V is the volume of electrolyte, t is the electrolysis time and m is the overall mass loading of electrocatalyst.

Faradaic efficiency (FE) was evaluated using the following equation:

$$FE = \left(3 \times F \times C_{NH3} \times V\right) / \left(17 \times Q\right)$$

Where F is the Faradaic constant, C_{NH3} is the detected concentration of ammonia, V is the volume of electrolyte and Q is the quantity of applied electricity.

Detection of hydrazine

The N_2H_4 by-product was detected by Watt and Chrisp method. 2.5 mL electrolyte after NRR measurement was mixed with 2.5 mL color reagent (a mixture of 5.99 g ρ-$C_9H_{11}NO$, 30 mL HCl and 300 mL C_2H_5OH), and then UV-vis spectrophotometer was performed within a range of 600 nm to 400 nm after standing at ambient conditions for 10 minutes. The N_2H_4 was characterized by the peaks at 455 nm.

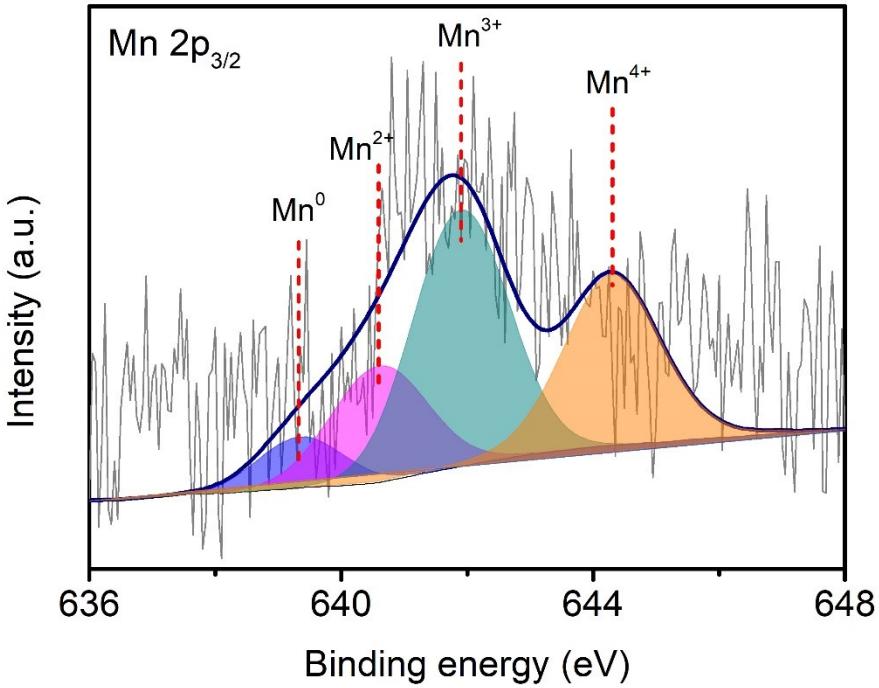

Fig. S1 High-resolution Mn $2p_{3/2}$ XPS spectrum of Mn_{SA}/GDY.

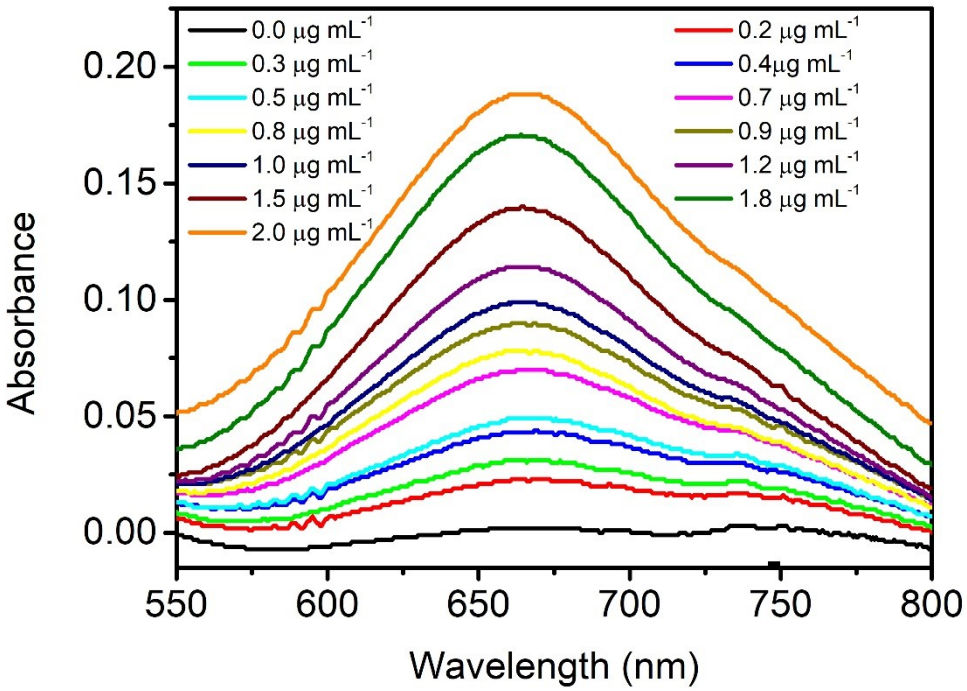

Fig. S2. UV-vis absorption spectra of indophenol assays with standard NH_4Cl solutions in 0.1 M Na_2SO_4 after 1 h incubation at room temperature

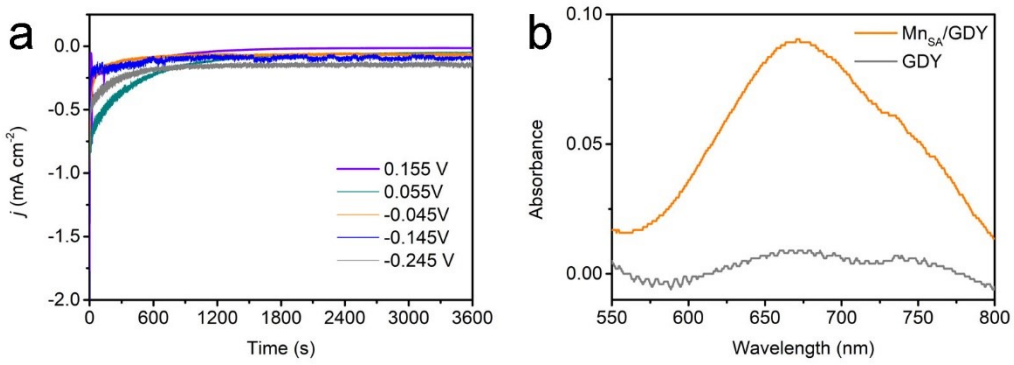

Fig. S3. (a) Chronoamperometry curves of Mn_{SA}/GDY tested at different potentials in 0.1 M Na_2SO_4. (b) UV-vis absorption spectra of the 0.1 M Na_2SO_4 electrolytes after NRR at -0.0.045 V versus RHE for Mn_{SA}/GDY and GDY.

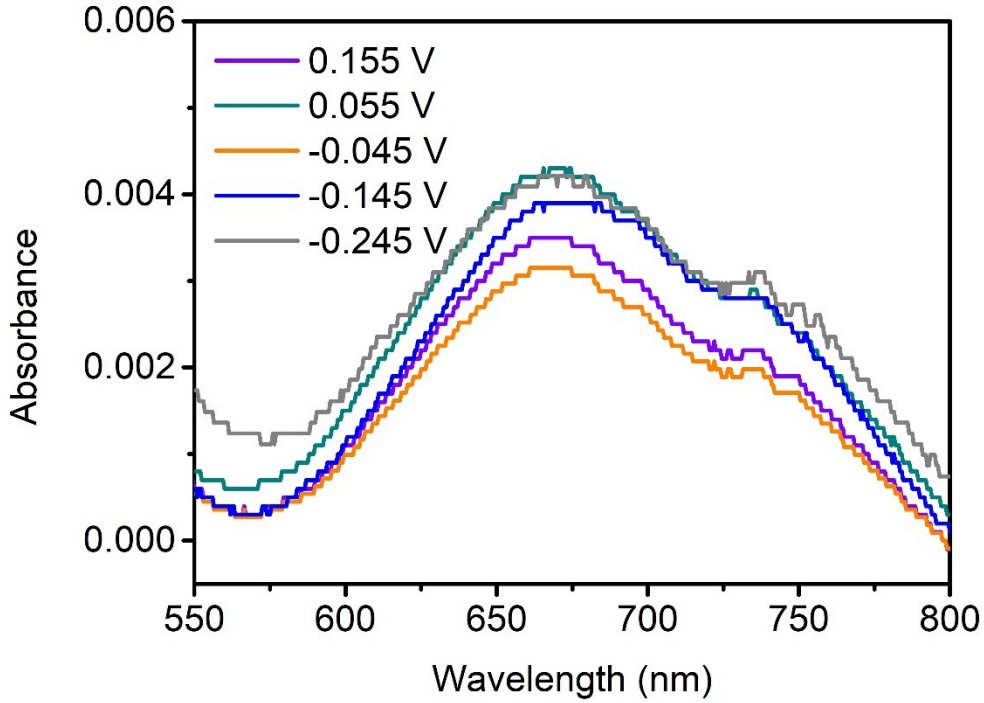

Fig. S4. UV-vis absorption spectra of the Ar-saturated 0.1 M Na_2SO_4 electrolytes after NRR at different applied potentials for Mn_{SA}/GDY.

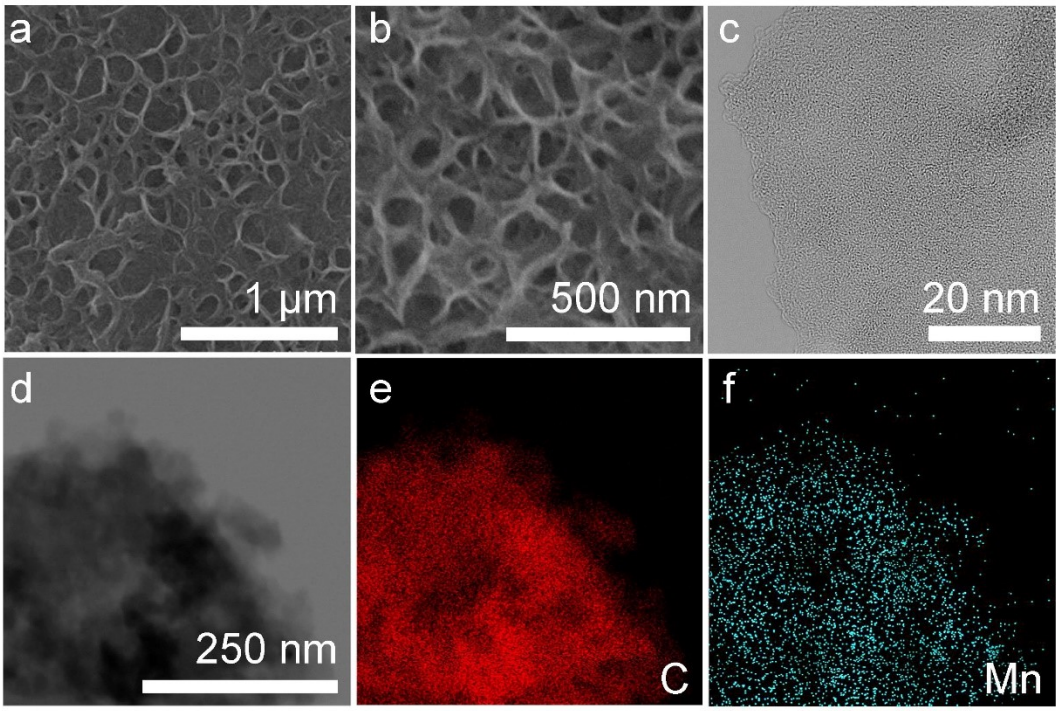

Fig. S5. (a-b) SEM images of Mn_{SA}/GDY after durability test. (c) High-resolution TEM image of Mn_{SA}/GDY after durability test. (d-f) STEM image and corresponding EDX elemental mapping results of Mn_{SA}/GDY after durability test

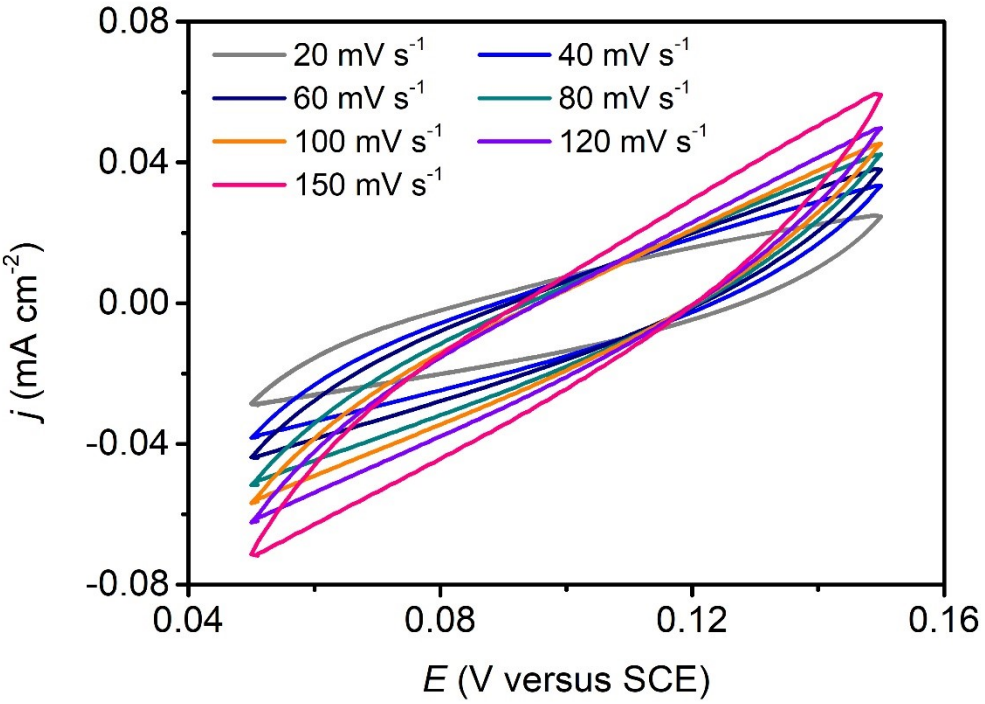

Fig. S6. CV curves of GDY recorded at different scan rates for C_{dl} estimation.

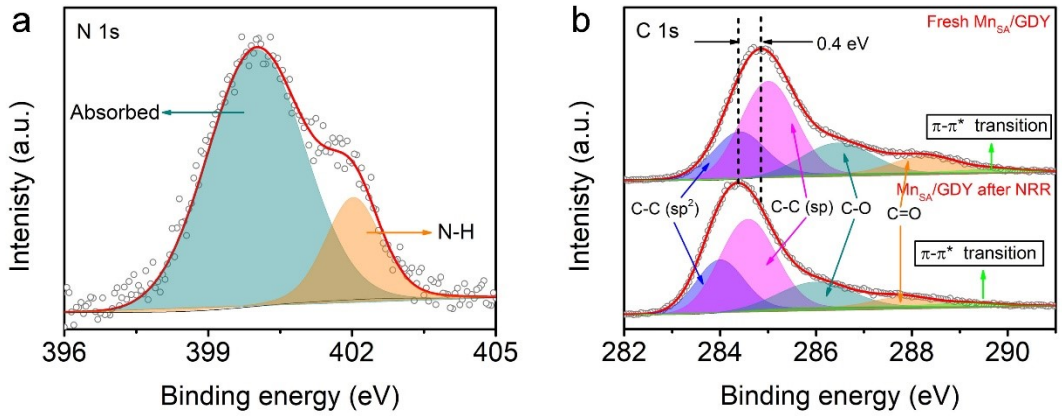

Fig. S7. (a) The N 1s XPS spectrum of Mn_{SA}/GDY after cycling stability test. (b) The C 1s XPS spectra of Mn_{SA}/GDY after cycling stability test.

The N 1s XPS spectrum of Mn_{SA}/GDY after cycling stability test was deconvoluted into two subpeaks attributed to the N-H bond absorbed N_2 respectively, which indicated the absorbance of N_2 and ammonia products as well as the corresponding intermediates on the surface of Mn_{SA}/GDY. The lower binding energy of C element of Mn_{SA}/GDY after nitrogen reduction reaction suggested the more electron-rich characteristic of GDY implying the trend of charge transfer from Mn atoms to GDY during electrocatalysis.

Table S1 Y_{NH3} and FE of Mn_{SA}/GDY for repetitive NRR tests at -0.045 V versus RHE in 0.1 M Na_2SO_4.

Repetitive time	**1**	**2**	**3**
Yield	44.02 μg h^{-1} $mg_{cat.}^{-1}$ (1.11e-10 mol s^{-1} cm^{-2})	45.24 μg h^{-1} $mg_{cat.}^{-1}$ (1.15e-10 mol s^{-1} cm^{-2})	46.78 μg h^{-1} $mg_{cat.}^{-1}$ (1.54 e-10 mol s^{-1} cm^{-2})
FE	35.53%	38.90%	39.83%

Table S2 Comparison of Y_{NH3} and FE of Mn_{SA}/GDY with previously reported electrocatalysts.

Electrocatalyst	**Yield**	**FE (%)**	**Ref.**
Mn_{SA}/GDY	46.78 μg h^{-1} $mg_{cat.}^{-1}$ (1.54e-10 mol s^{-1} cm^{-2})	39.83	This work
SA Ru-Mo_2CT_x	40.57 μg h^{-1} $mg_{cat.}^{-1}$	25.77	[1]
Zn/Fe-N-C	30.5μg h^{-1} $mg_{cat.}^{-1}$	26.5	[2]
Mn-N-C SAC	21.43μg h^{-1} $mg_{cat.}^{-1}$	32.02	[3]
Fe_{SA}-NO-C	31.9μg h^{-1} $mg_{cat.}^{-1}$	11.8	[4]
Ru SAs/g-C_3N_4	23.0μg h^{-1} $mg_{cat.}^{-1}$	8.3	[5]
Zr-TiO_2	8.9 μg h^{-1} cm^{-2}	17.3	[6]
C-Ti_xO_y/C	14.8μg h^{-1} $mg_{cat.}^{-1}$	17.8	[7]
$W_{18}O_{49}$-16Fe	24.7μg h^{-1} $mg_{cat.}^{-1}$	20.0	[8]
Ru_2P-rGO	32.8μg h^{-1} $mg_{cat.}^{-1}$	13.04	[9]
Cu/PI-300	17.2μg h^{-1} cm^{-2}	6.56	[10]
Co-MoS_{2-x}	5.44μg h^{-1} $mg_{cat.}^{-1}$	1.7	[11]

Table S3 Impedance parameters derived from the fitted equivalent circuit for the impedance spectra recorded in 0.1 M Na_2SO_4.

Electrocatalyst	**Mn_{SA}/GDY**	**GDY**
R_s (ohm)	13.44	13.8
CPE1, Yo (S-sec^n)	1.66e-3	3.10e-2
n	0.56	0.47
Rct (ohm)	2.41	3.41
CPE2, Yo (S-sec^n)	5.53e-4	3.34e-3
n	0.79	0.94
R_a (ohm)	882.70	560.90

Table S4 Yields and FEs of Mn_{SA}/GDY with different Mn atoms mass loading.

Mass loading (wt. %)	**Yield (μg h^{-1} $mg_{cat.}^{-1}$)**	**FE (%)**
0.19	46.78 μg h^{-1} $mg_{cat.}^{-1}$	39.83
0.10	28.03 μg h^{-1} $mg_{cat.}^{-1}$	27.74
0.07	11.69 μg h^{-1} $mg_{cat.}^{-1}$	19.51

References

1. W. Peng, M. Luo, X. Xu, K. Jiang, M. Peng, D. Chen, T. Chan and Y. Tan, *Adv. Energy Mater*., 2020, **10**, 2001364.
2. L. Zhang, G. Fan, W. Xu, M. Yu, L. Wang, Z. Yan and F. Cheng, *Chem. Commun*., 2020, **56**, 11957-11960.
3. X. Wang, D. Wu, S. Liu, J. Zhang, X. Fu and J. Luo, *Nano-Micro Letter*, 2021, **13**, 125.
4. Y. Li, J. Li, J. Huang, J. Chen, Y. Kong, B. Yang, Z. Li, L. Lei, G. Chai, Z. Wen, L. Dai, and Y. Hou, *Angew. Chem. Int. Ed*., 2021, **60**, 9078-9085.
5. B. Yu, H. Li, J. White, S. Donne, J. Yi, S. Xi, Y. Fu, G. Henkelman, H. Yu, Z. Chen and T. Ma, *Adv. Funct. Mater.*, 2020, **30**, 1905665.
6. N. Cao, Z. Chen, K. Zang, J. Xu, J. Zhong, J. Luo, X. Xu and G. Zheng, *Nat. Commun*., 2019, **10**, 2877.
7. Q. Qin, Y. Zhao, M. Schmallegger, T. Heil, J. Schmidt, R. Walczak, G. Gescheidt-Demner, H. Jiao and M. Oschatz, *Angew. Chem. Int. Ed*., 2019, **58**, 13101-13106.
8. R. Zhao, C. Liu, X. Zhang, X. Zhu, P. Wei, L. Ji, Y. Guo, S. Gao, Y. Luo, Z. Wang and X. Sun, *J. Mater. Chem. A*, 2020, **8**, 77.
9. Y. Tong, H. Guo, D. Liu, X. Yan, P. Su, J. Liang, S. Zhou, J. Liu, G. Lu and S. Dou, *Angew. Chem. Int. Ed*., 2020, **59**, 7356-7361.
10. Y. Lin, S. Zhang, Z. Xue, J. Zhang, H. Su, T. Zhao, G. Zhai, X. Li, M. Antonietti and J. Chen, *Nat. Commun*., 2019, **10**, 4380.
11. J. Zhang, X. Tian, M. Liu, H. Guo, J. Zhou, Q. Fang, Z. Liu, Q. Wu and J. Lou, *J. Am. Chem. Soc.*, 2019, **141**, 19269-19275.